Combining Genetic and Gravitational Search Algorithms for the Optimal Management of Battery Energy Storage Systems in Real-Time Pricing Markets

Juan M. Lujano-Rojas, José M. Yusta, José A. Domínguez-Navarro
University of Zaragoza
Zaragoza, Spain
lujano.juan@gmail.com; {jmyusta; jadona}@unizar.es

Gerardo J. Osório
C-MAST, University of Beira Interior
Covilha, Portugal
gjosilva@gmail.com

Miadreza Shafie-khah
School of Technology and Innovations University of Vaasa
Vaasa 65200, Finland
mshafiek@univaasa.fi

Fei Wang
Department of Electrical Engineering North China Electric Power University
Baoding 071003, China
feiwang@ncepu.edu.cn

João P. S. Catalão
Faculty of Engineering of the University of Porto and INESC TEC
Porto, Portugal
catalao@fe.up.pt

2020 IEEE Industry Applications Society Annual Meeting | 978-1-7281-7192-0/20/$31.00 ©2020 IEEE | DOI: 10.1109/IAS44978.2020.9334858

***Abstract*—Determining the optimal management in terms of operative decisions (charging, discharging, or disconnection) as well as their magnitudes (charging/discharging current/power), considering the nonlinearities of battery energy storage system (BESS) is a crucial process on the successful acceptance of energy storage technologies. This work presents an optimization model for the management of BESS operating in real-time electricity markets in order to maximize the economic profits by energy arbitrage. The optimization model proposed combines genetic algorithm (GA) with gravitational search algorithm (GSA). On one hand, GA uses an integer codification, where charging, discharging, and disconnection are represented. On the other hand, GSA optimizes the maximum charging or discharging energy. The proposed combination of optimization algorithms allows determining the integer and continuous variables involved in the management problem, taking into account the nonlinear behavior of BESS. The proposed approach was implemented considering lead acid and vanadium redox flow batteries under the conditions of Spanish electricity market.**

***Keywords*—Battery energy storage system, Genetic algorithm, Gravitational search algorithm, Lead acid battery, Vanadium redox flow battery.**

I. NOMENCLATURE

$\vec{a}_{GSA}^{opt}$, $\vec{b}_{GA}^{opt}$	Near-optimal solution for GSA and GA, respectively.
$a_{(r,\theta)}$, $a_{(1,\theta)}^{opt}$	Position of mass r and the heaviest one, respectively.
$\vec{a}_{(r)}$, $\vec{b}_{(i)}$	Mass r (GSA) and i (GA), respectively.
B	GA population matrix.
$b_{(i,t)}$	Element of individual i and time t.
C_N	BESS capacity (Ah/cell or kWh/cell).
ε_{min}, ε_{max}	Position limits between two masses.
$E_{(t)}$	Electricity price at time t (€/kWh).
$\eta_{B(t)}$, $\eta_{C(t)}$	Battery and converter efficiencies at time t, respectively.
$\eta_{(t)}^{C}$, $\eta_{(t)}^{D}$	VRFB charging and discharging efficiencies at time t, respectively.
$\eta_{V(t)}^{C}$, $\eta_{E(t)}^{C}$	VRFB voltage and energy efficiencies at time t for charging, respectively.
$\eta_{V(t)}^{D}$, $\eta_{E(t)}^{D}$	VRFB voltage and energy efficiencies at time t for discharging, respectively.
$f_{GA(i)}$, $f_{GSA(r)}$	Fitness of individual i and mass r, respectively.
f_{GA}^{max}	Highest fitness value (GA).
f_{GSA}^{min}, f_{GSA}^{max}	Mass limits of GSA.
$g_{GSA(r)}$	GSA mutation function for mass r.
$H_1^C - H_9^C$	Parameters of LAB-voltage.
$H_1^D - H_5^D$	
i	Index for GA individual ($i = 1, \dots, I$).
$I_{B(t)}$, $P_{B(t)}$	LAB-current (A/cell) and VRFB-power (kW/cell) at time t, respectively.
$I_{G(t)}$	Gassing current at time t (A/cell).
$I_{M(t)}$, $P_{M(t)}$	Dispatch limits (Ah/cell or kWh/cell).
$K_1^C - K_{15}^C$	Parameters of VRFB-voltage.
$K_1^D - K_{12}^D$	
L_1^C, L_2^C	Parameters of power converter.
$P_{C(t)}$	Power of converter at time t (kW).
P_N, I_N	Rating VRFB (kW/cell) and LAB (A/cell) parameters, respectively.
r	Index GSA mass ($r = 1, \dots, R$).
$RND_{con}(0,1)$	Continuous random number in [0,1].
$RND_{int}(1,T)$	Integer random number in [1,T].
SOC_B^{min}, SOC_B^{max}	SOC limits, respectively.
$SOC_{(t)}$, $DOD_{(t)}$	SOC and DOD at time t, respectively.
t	Index for each time step ($t = 1, \dots, T$).
θ, δ	Integer and continuous numbers.
V_B^{min}, V_B^{max}	Voltage limits (V/cell).

$V_{B(t)}$ BESS voltage at time t (V/cell).

II. Introduction

Preservation of natural resources, against the intensive industrial development, is currently an objective with high priority. Worldwide, renewable energies are being intensively adopted in order to reach the environmental goals. However, the intrinsic variability from renewable resources represents important barriers to be fully adopted. Increasing power system flexibility would be appropriate in order to increase the energy consumption from renewable resources in a feasible manner. In these regards, the flexibility could be improved by embracing, e.g. some demand response programs or by adopting battery energy storage system (BESS) technologies.

Management of BESS is an important problem due to its influence on the techno-economic performance of energy systems. BESS sizing and management consists on the solution of an optimization problem formulated in order to maximize the system revenue under a determined pricing scheme (real-time pricing or time-of-use tariff), or by minimizing the net present cost over a determined lifetime.

Typically, the optimization problem can be solved using linear programming (LP), nonlinear (NLP), mixed-integer linear programming (MILP), mixed-integer nonlinear programming (MINLP), robust optimization (RO), dynamic programming (DP), genetic algorithm (GA), optimal control, among other techniques. In general sense, the optimization technique depends on the type of the model implemented and the energy policy under consideration [1]. In this regard, for instance in [2] was presented a management model combining RO and MILP. The uncertainties of the available budget as well as the degradation of the BESS were incorporated, specifically for valve-regulated lead-acid batteries (LABs) and lithium-ion (LI) batteries.

In [3] was proposed a management algorithm for reducing the variability of photovoltaic (PV) generation and energy time shifting. The model consisted of estimating a reference PV-generation curve, BESS capacity, and its state-of-charge (SOC). This process was carried out by the feature computation of the PV-power production reference, and by computing the smoothed maximum PV-power curve, detecting the PV-power intermittency.

In [4] was developed an optimization model under the concept of hybrid BESS (HBESS). The studied configuration consisted of the main bank, installed for the long-term storage, and the secondary bank, installed for short-term or balancing operation. In a global perspective, this configuration resulted in an effective usage of storage devices, extending the battery lifetime. Additionally, a management and sizing strategy was proposed based on a probability theory, in order to find a cost-effective configuration by reducing the fuel-consumption cost.

Similarly, in [5] was created a model for sizing and optimize the HBESS, formulated as a MINLP problem. Following this topic, in [6] was developed a technique based on a two-stage control approach to stabilize the system voltage, while reducing the BESS degradation. In [7] was developed a multi-objective optimization model based on Radau pseudospectral methodology. The different variables of the model were represented using a Lagrange polynomial interpolation, so that the system management is carried out using NLP.

In [8] was developed an optimization model based on DP, which uses specific models of LI and vanadium redox flow batteries (VRFBs), in order to increase the accuracy of the optimization process. The capabilities of the optimization model were illustrated by maximizing the revenue of a BESS, operating in PJM electricity market. In [9] was created a computational model involving the optimal sizing and management of BESS in a multiscale manner. Specifically, the model accounted with the decisions, made in minutes, and with the replacement decisions, made in years, where the loss capacity and BESS degradation were taken into account. To this end, a multiscale LP approach was presented in order to determine the optimal BESS usage, and to presents the profitability of a BESS enrolled in the ancillary service markets, assessing the importance of the BESS-degradation process against the system profitability.

In [10] was presented an optimization strategy, implemented in two different levels, to manage a central and a distributed BESS (DBESS), as well as a shunt capacitor. The central and DBESS provided ancillary services on a centralized and distributed manner, respectively. During the first level, DBESS were optimally located to minimize the energy losses, while during the second level, the distributed devices were optimally operated considering reverse power flow and load deviations, among others technical constraints.

In [11] was developed a sizing BESS model based on Markov process. The model aimed to determine the optimal size of the BESS in order to maximize the economic benefits. To this end, the Markov states were determined using a fuzzy-c-means algorithm, while the optimization problem was solved using interior-point algorithm. In [12] was developed a model able to overcome the main limitations of Q-learning methods for the energy system management. The model considered the uncertainty sources as well as the overestimation mitigation of the traditional Q-learning technique. As can be observed from the presented overview, the analysis of the BESS managing models is a widespread, challenging and innovative researching field. The simulation and the optimization of BESS is a key topic toward the massive incorporation of renewable power sources such as PV and wind generation. In this sense, this work is an extension of a previous optimization technique developed in [13].

The proposed technique is based on an integer-coded GA, where charging, discharging, and disconnection are represented using integer number, +1, –1, and 0, respectively. During the charging and discharging conditions, the BESS was assumed to be operated at its maximum current per cell. In other words, the variables under optimization were only the integer decision variables aforementioned. Given the importance of the storage technology and the accuracy of its simulation model, two storage technologies have been considered, LAB and VRFB, specifically.

In the extension presented in this work, integer decision variables as well as the maximum current (LAB) and the power (VRFB) per cell are simultaneously considered during the optimization process. To achieve this goal, the GA formulation proposed in [13] has been combined with a simplified version of gravitational search algorithm (GSA) in

order to incorporate the current and the power optimization as a continuous variable.

The rest of the paper is organized as follow: Section III briefly describes the mathematical model of LAB and VRFB, Section IV presents the proposed management strategy based on the combination of GA and GSA; Section V illustrates the proposed model by analyzing a case study. Finally, the main conclusions and remarks are discussed in Section VI.

III. Battery Energy Storage System Simulation

Fig. 1 shows a simplified diagram of BESS under study. It is connected to the wholesale electricity market using the smart meter and the advanced measurement infrastructure of smart grid. As explained before, two different technologies have been considered, LAB and VRFB, specifically.

In the case of VRFB, energy management system (EMS) requires of the rating capacity (C_N), rating power of cell-stack (P_N), and other parameters related to the voltage and SOC during charging ($K_1^C - K_{15}^C$) and discharging ($K_1^D - K_{12}^D$) processes, respectively.

Moreover, EMS requires of the rating capacity (C_N) and rating current (I_N) as well as LAB simulation parameters for charging ($H_1^C - H_9^C$) and discharging ($H_1^D - H_5^D$) processes, respectively.

Simulation parameters of power converter (L_1^C, L_2^C) are also required due to the influence of its efficiency on the power imported/exported to the grid. The number of storage units connected in serial and parallel gives an idea about how battery bank is scaled.

EMS determines if BESS should be charged, discharged, or disconnected, and the optimal charging or discharging power (VRFB) or current (LAB), depending on the technology under analysis. EMS collects hourly values of electricity prices ($E_{(t)}\ \forall t = 1, \dots, T$) in order to perform the corresponding day-ahead (T=24h) forecast.

Simultaneously, EMS measures the state of BESS in terms of voltage ($V_{B(t)}$), current ($I_{B(t)}$), power ($P_{B(t)}$), and SOC ($SOC_{B(t)}$). All of this information is used by EMS to evaluate the proposed GA-GSA in order to determine the optimal state (battery charging, discharging, or disconnection) as well as the optimal power ($P_{M(t)}\ \forall t = 1, \dots, T$) or the current ($I_{M(t)}\ \forall t = 1, \dots, T$), depending on the BESS-technology. Next subsection describes the models, for the LAB (Subsection A) and the VRFB model (Subsection B), implemented in this work.

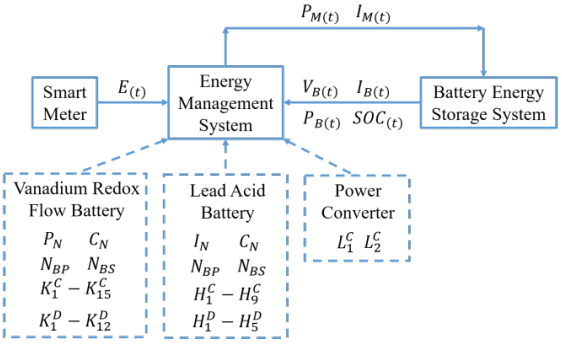

Figure 1. Scheme of BESS operation.

A. Lead Acid Battery Model

The simulation model for LAB used in this work was proposed in [14]. Charging and discharging processes and the SOC-estimation are presented in (1)-(4). This model was developed by modifying the Shepherd's equations. The model considers the behavior of open-circuit voltage with SOC, the ohmic losses as well as the overvoltage typically observed when SOC is close to one. The charging voltage estimation ($V_{B(t)}$) is carried out using (1), while the gassing current ($I_{G(t)}$) is presented in (2), and the discharging voltage is shown in (3). Finally, SOC is calculating according to (4), where the effect of gassing process is considered.

$$V_{B(t)} = H_1^C - H_2^C\left(DOD_{(t)}\right) + H_3^C\left(\frac{I_{B(t)}}{C_N}\right) + H_4^C\left(\frac{I_{B(t)}}{C_N}\right)\left(\frac{SOC_{(t)}}{H_5^C - SOC_{(t)}}\right), \quad I_{B(t)} > 0\ \forall t = 1, \dots, T. \tag{1}$$

$$I_{G(t)} = C_N H_6^C exp\left(H_7^C\left[V_{B(t)} - H_8^C\right] + H_9^C\right),\ \forall t = 1, \dots, T. \tag{2}$$

$$V_{B(t)} = H_1^D - H_2^D\left(DOD_{(t)}\right) + H_3^D\left(\frac{I_{B(t)}}{C_N}\right) + H_4^D\left(\frac{I_{B(t)}}{C_N}\right)\left(\frac{DOD_{(t)}}{H_5^D - DOD_{(t)}}\right), \quad I_{B(t)} \le 0\ \forall t = 1, \dots, T. \tag{3}$$

$$SOC_{(t)} = SOC_{(t-1)} + \int_0^\tau \left(\frac{I_{B(t)} - I_{G(t)}}{C_N}\right) d\tau,\ \forall t = 1, \dots, T. \tag{4}$$

B. Vanadium Redox Flow Battery Model

The model of the VRFB implemented in this work is based on [15-17]. It was formulated using the information from experimental tests. The battery efficiency is defined in (5) including charging ($P_{B(t)} > 0$) and discharging ($P_{B(t)} < 0$) processes, respectively. Charging process in described in (6-9). The behavior of the voltage as a function of the SOC ($SOC_{(t)}$) and the charging power ($P_{B(t)}$) is explained in (6).

Voltage and energy efficiencies ($\eta_{V(t)}^C$ and $\eta_{E(t)}^C$) during the charge are shown in (7) and (8), respectively. These expressions are used to calculate charging efficiency ($\eta_{(t)}^C$) in (9). The discharging process is presented in (10-13); the voltage variation with the SOC and the discharging power is shown in (10).

The voltage and the energy efficiencies ($\eta_{V(t)}^D$ and $\eta_{E(t)}^D$) are explained in (11) and (12), respectively. Moreover, the discharging efficiency ($\eta_{(t)}^D$) is shown in (13). Finally, the SOC-estimation is presented in (14), which is formulated as a function of instantaneous VRFB power and efficiency.

$$\eta_{B(t)} = \begin{cases} \eta_{(t)}^C;\ P_{B(t)} > 0 \\ \eta_{(t)}^D;\ P_{B(t)} < 0 \end{cases}, \qquad \forall t = 1, \dots, T \tag{5}$$

$$V_{B(t)} = \left(K_1^C SOC_{(t)} + K_2^C\right)P_{B(t)} + K_3^C SOC_{(t)} + K_4^C, \quad \forall t = 1, \dots, T; \tag{6}$$

$$\eta_{V(t)}^C = \frac{K_5^C T_E\left(SOC_{(t)} - K_6^C\right) + K_7^C}{\left(K_8^C SOC_{(t)} + K_9^C\right)P_{B(t)} + K_{10}^C SOC_{(t)} + K_{11}^C}, \quad \forall t = 1, \dots, T; \tag{7}$$

$$\eta^{C}_{E(t)} = \frac{\left(K^{C}_{12} SOC_{(t)} + K^{C}_{13}\right) P_{B(t)} + K^{C}_{14} SOC_{(t)} - K^{C}_{15}}{P_{B(t)}}, \quad \forall\, t = 1, \dots, T; \tag{8}$$

$$\eta^{C}_{(t)} = \eta^{C}_{V(t)} \eta^{C}_{E(t)}, \qquad \forall\, t = 1, \dots, T. \tag{9}$$

$$V_{B(t)} = K^{D}_{1} \left| P_{B(t)} \right| + K^{D}_{2} SOC_{(t)} + K^{D}_{3}, \qquad \forall\, t = 1, \dots, T; \tag{10}$$

$$\eta^{D}_{V(t)} = \frac{K^{D}_{4} \left| P_{B(t)} \right| + K^{D}_{5} SOC_{(t)} + K^{D}_{6}}{K^{D}_{7} T_{E} \left(SOC_{(t)} - K^{D}_{8} \right) + K^{D}_{9}}, \qquad \forall\, t = 1, \dots, T; \tag{11}$$

$$\eta^{D}_{E(t)} = \frac{|P_{B(t)}|}{K^{D}_{10} |P_{B(t)}| + K^{D}_{11} SOC_{(t)} (SOC_{(t)} - 1) + K^{D}_{12}}, \quad \forall\, t = 1, \dots, T; \tag{12}$$

$$\eta^{D}_{(t)} = \eta^{D}_{V(t)} \eta^{D}_{E(t)}, \qquad \forall\, t = 1, \dots, T; \tag{13}$$

$$SOC_{(t)} = SOC_{(t-1)} + \int_{t-1}^{t} \left(\frac{P_{B(t)} \eta_{B(t)}}{C_N} \right) d\tau, \quad \forall\, t = 1, \dots, T. \tag{14}$$

C. Power Converter Model

The influence of power converter on the BESS performance is modeled using its efficiency, which is calculated by (15). Then, the value of the power through the converter is calculated using (16). This model is a simplification of the models suggested in [18].

$$\eta_{C(t)} = \frac{P_{B(t)}}{L^{C}_{1}(P_N) + (1 + L^{C}_{2}) P_{B(t)}}, \qquad \forall\, t = 1, \dots, T; \tag{15}$$

$$P_{C(t)} = \pm \frac{\left| P_{B(t)} \right| - L^{C}_{1}(P_N)}{1 + L^{C}_{2}}, \qquad \forall\, t = 1, \dots, T. \tag{16}$$

IV. Battery Energy Storage System Simulation

As described in Fig. 1, EMS determines the optimal operation of the BESS by incorporating the corresponding simulation model, which depends on the technology under study (LAB or VRFB), on an optimization model to determine the operative decisions (battery charging, discharging or disconnection) and the charging or discharging power of VRFB or the current of LAB. On one hand, operative decisions are represented by using integer variables. On the other hand, the power or the current dispatch are represented by using continuous variables. Under these circumstances, the optimal management can be formulated as MINLP problem, solved by means of the combination of heuristic techniques (GA and GSA), which is the main contribution of this work.

A. Optimization of the Battery Operative Decisions

As previously mentioned, the battery charging, discharging, and disconnection are operative decisions represented by using integer variables, +1, –1, and 0, respectively. The appropriate selection of these variables are carried out by using the integer-coded GA. GA-population (B) is shown in (17), which is a matrix whose rows are the GA-individuals ($\vec{b}_{(i)}\ \forall\, i = 1, \dots, I$), represented in (18). The length of this vector is the time horizon of the optimization method (one day or $T = 24h$).

The definition of each element of the GA-population is described in (19), which is defined according to the technology under consideration (LAB or VRFB) for the three main decisions. The fitness of each GA-individual is evaluated according to (20), while the best individual ($\vec{b}^{\,opt}_{GA}$), during a determined generation (GA iteration), is determined by the maximum fitness (f^{max}_{GA}) as explained in (21) and (22). During each iteration (generation), the crossover and mutation operators are performed over the GA-population, and the information related to the characteristics of the individual with highest fitness is kept on the track.

$$B = \left[\vec{b}_{(1)} \dots \vec{b}_{(i)} \dots \vec{b}_{(I)} \right]^{T} \tag{17}$$

$$\vec{b}_{(i)} = [b_{(i,1)} \quad \cdots \quad b_{(i,t)} \quad \cdots \quad b_{(i,T)}], \qquad \forall\, i = 1, \dots, I; \tag{18}$$

$$b_{(i,t)} = \begin{cases} +1;\ I_{(t)} > 0\ or\ P_{(t)} > 0 \\ -1;\ I_{(t)} < 0\ or\ P_{(t)} > 0 \\ 0;\ I_{(t)} = 0\ or\ P_{(t)} = 0 \end{cases}, \forall\, i = 1, \dots, I; t = 1, \dots, T; \tag{19}$$

$$f_{GA(i)} = \frac{I + 1 - i}{\sum_{l=1}^{I} \{I + 1 - l\}}, \qquad \forall\, i = 1, \dots, I; \tag{20}$$

$$f^{max}_{GA} = max\{ f_{GA(i)}\ \forall\, i = 1, \dots, I \}; \tag{21}$$

$$\vec{b}^{\,opt}_{GA} = \vec{b}_{(i)} \mid f_{GA(i)} = f^{max}_{GA}. \tag{22}$$

B. Optimization of the Battery Power Dispatch

The charging and discharging power of VRFB and the current of LAB are optimized by means of a simplified version of the original GSA [19]. The position of a determined mass (r) in a dimension (t) is represented by a continuous variable ($a_{(r,t)}$), the position of an object (r) is represented by a vector ($\vec{a}_{(r)}$), with T columns and only 1 row, where each element is the aforementioned variable $a_{(r,t)}$ with $r \in [1, R]$, and $t \in [1, T]$. With respect to the battery management problem, the variable $a_{(r,t)}$ is the maximum power of VRFB or the current LAB per cell to be applied during the charging and discharging process at each time step t, respectively. Initially a determined amount of masses (R) is defined. Then, the weight of each mass is calculated according to (23).

After that, the maximum and minimum weight is determined as suggested in (24) and (25), respectively, and the object with highest mass or near-optimal solution ($\vec{a}^{\,opt}_{GSA}$) is identified as expressed in (26). Depending on the distance between each mass from the heaviest one, GSA modifies the coordinates ($a_{(r,t)}$) of each mass so that lightest masses are attracted to the heaviest one. The manner in which the position of each mass should be modified is defined according to (27).

The variable $g_{GSA(r)}$ is an integer on the interval [1, T], representing the column of the vector $\vec{a}_{(r)}$ that should be modified. Note that for the heaviest object ($f_{GSA(r)} = f^{max}_{GSA}$), $g_{GSA(r)}$ is equal to zero, which means that no column of $\vec{g}_{GSA(r)}$ should be altered. On the contrary case, for the lightest object ($f_{GSA(r)} = f^{max}_{GSA}$) $g_{GSA(r)}$ is equal to T, which means that all of the columns of vector $\vec{a}_{(r)}$ should be modified.

The dimension to be modified (t) is selected using an integer random number generator (RND_{int}) in the interval [1, T], while the position $a_{(r,t)}$ is modified using a continuous random number generator (RND_{con}) in the interval [0, 1]. The implementation of the GSA as a mutation operator is presented in Fig. 2. This algorithm is repeated during each iteration (actual age of the universe) of the GSA, as the position of heaviest object remains unchanged. The algorithm only keeps track of the best solution during each iteration.

$$f_{GSA(r)} = \frac{R + 1 - r}{\sum_{l=1}^{R} \{R + 1 - l\}}, \qquad \forall\, r = 1, \dots, R; \tag{23}$$

$$f_{GSA}^{min} = min\{f_{GSA(r)}\ \forall\, r = 1, \dots, R\}; \quad (24)$$

$$f_{GSA}^{max} = max\{f_{GSA(r)}\ \forall\, r = 1, \dots, R\}; \quad (25)$$

$$\vec{a}_{GSA}^{opt} = \vec{a}_{(r)} \mid f_{GSA(r)} = f_{GSA}^{max}; \quad (26)$$

$$g_{GSA(r)} = INT\left(\left[1 - \frac{f_{GSA(r)} - f_{GSA}^{min}}{f_{GSA}^{max} - f_{GSA}^{min}}\right] T\right), \quad \forall\, r = 1, \dots, R. \quad (27)$$

C. Management Algorithm for the Day-Ahead Operation

Management of BESS consists of the solution of an optimization problem in which specific characteristics of the LAB and the VRFB are considered. This problem consists of the simulation models of Section III combined with the objective function defined in (28) and constraints shown in (29)-(33), depending on the technology adopted.

$$min\left\{\sum_{t=1}^{T} P_{C(t)} E_{(t)}\right\}; \quad (28)$$

subject to:

$$V_B^{min} \le V_{B(t)} \le V_B^{max}, \quad \forall\, t = 1, \dots, T; \quad (29)$$

$$0 \le I_{B(t)} \le I_N, \quad \forall\, t = 1, \dots, T; \quad (30)$$

or:

$$0 \le P_{B(t)} \le P_N, \quad \forall\, t = 1, \dots, T; \quad (31)$$

$$0 \le P_{C(t)} \le P_N, \quad \forall\, t = 1, \dots, T; \quad (32)$$

$$SOC_B^{min} \le SOC_{(t)} \le SOC_B^{max}, \quad \forall\, t = 1, \dots, T; \quad (33)$$

Daily revenue is represented in (28), having to be minimized, since the discharged or sold power is defined negative. In this sense, the net transaction in T = 24h between BESS and the grid should be negative in order to get some economic benefit. Constraint (29) is the operative constraint imposed by the BESS manufacturer. Constraints (30) and (31) are the limits for the battery current LAB and the battery power VRFB, respectively. Constraint (32) is the operative limit of power converter, assuming its rated power equal to the rating power of BESS.

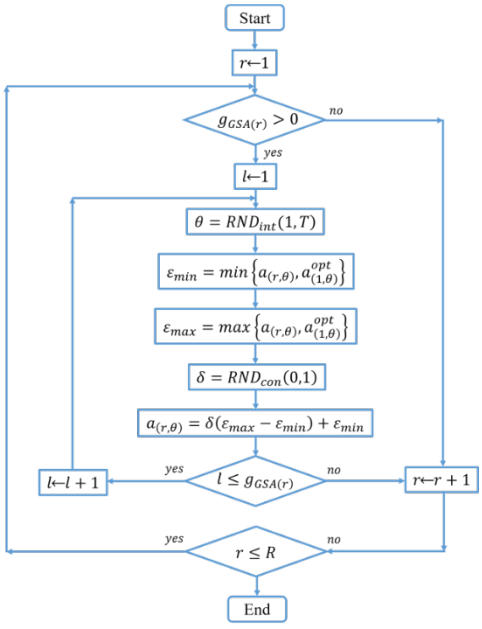

Figure 2. Algorithm for simplified-GSA implementation.

Finally, constraint (33) corresponds to the limitation of the SOC applied to both technologies, LAB and VRFB, respectively. In the case of the LAB, $V_{B(t)}$ is calculated using (1) and (3) for the charging and discharging, respectively. For the VRFB, it is calculated using (6) and (10), for the charging and discharging, respectively. The maximum LAB current is a variable to be optimized by the EMS considering the constraint (30). Similarly, the maximum VRFB power is a variable to be optimized by the EMS considering the constraint (31). Once a determined value of the battery power has been considered, the influence of the power converter is introduced by calculating the power flowing using (16). Finally, the SOC required to evaluate the constraint (33) is calculated using (4) for the LAB and (14) for the VRFB.

The optimization problem can be solved by performing the simultaneous optimization of the battery operative decisions and power dispatch. It can be carried out by combining GA and GSA and following the structure defined in Fig. 2 and the model described in Section 3. Initial population of GA (B) is created using integer random numbers. Then, the fitness of each individual ($\vec{b}_{(i)}$) is obtained as a result of GSA.

This procedure is then repeated for all of the GA-individuals until a determined number of iterations (generations) is reached, resulting in the near-optimal solution ($\vec{b}_{GA}^{opt}$) of the problem. This is the manner how GA and GSA interact between each other. Finally, the maximum charging and discharging current ($I_{M(t)}\ \forall\, t = 1, \dots, T$), or power ($P_{M(t)}\ \forall\, t = 1, \dots, T$) are defined by $\vec{a}_{GSA}^{opt}$, while the operative decisions are defined by the vector $\vec{b}_{GA}^{opt}$.

V. Case Study

The electricity prices of the Spanish market during the year 2018 were used. The time series between September 1st and 30th were used to predict the prices of October 1st, which is the day under study. A feedforward neural network with 50 hidden layers was trained, taking as input the last 168 hourly values (one week). Fig. 3 shows the actual and predicted values. The proposed algorithm is applied using this predicted profile; then, the solution is evaluated over the actual price profile in order to obtain the information about the effects of the prediction errors on the net benefit estimation.

Two different systems are analyzed, one using a LAB, and another one using a VRFB. The system based on the LAB uses cells of 2500 Ah (C_N=2500 Ah). Each cell has a maximum current of 250 A (I_N=250 A), minimum SOC of 0.3 (SOC_B^{min}=0.3), maximum SOC of 1 (SOC_B^{max}=1). With respect to voltage limitations, V_B^{min}=1.95 V/cell and V_B^{max}=2.23 V/cell were considered. The bank is composed of 10 cells connected in serial and 100 connected in parallel. The parameters of the simulation model can be found in [14].

The system based on the VRFB uses cells of 5 kW/20 kWh (P_N=5 kW and C_N=20 kWh). The parameters of these cells are published in [15-17]. The bank is composed of 100 cells connected in serial and 150 cells connected in parallel. Minimum SOC of 0.15 (SOC_B^{min}=0.15), maximum SOC of 0.9 (SOC_B^{max}=0.9), were considered. With respect to the voltage limitations, $V_B^{min} = 42$ V/cell and $V_B^{max} = 56.5$ V/cell were considered.

For the analysis of both systems, GA-parameters were adjusted to the same values, population of 85 individuals, 150 generations, crossover rate of 90%, and mutations rate of 5%, respectively. However, GSA-parameters were adjusted differently for the LAB and the VRFB in order to compensate for the complexity of the computational models implemented, in special for the VRFB. The GSA implemented to optimize the LAB-current was performed considering 85 masses and 150 iterations (age of the universe). Moreover, the GSA used for the VRFB power management was evaluated using 25 masses and 100 iterations. The results for the LAB and the VRFB were obtained in MATLAB® with a standard computer with i7-363QM CPU at 2.4 GHz, 8 GB of RAM and a 64-bit operating system. Table I shows the net benefit under the predicted and actual conditions. According to these results, the prediction error introduces uncertainty between 0.9% and 15.6% on the net benefit estimation.

The computational time required was between 13.06 minutes and 15.45 minutes, for the LAB and the VRFB, analysis, respectively. Fig. 4 shows the power profile per technology during the day under analysis. The price signal was added for the sake of understanding. Together with previous results, Fig. 5 presents the SOC profile for both technologies, and Table II shows the current and power signals at each time step, as well as the operative decisions regarding charging, discharging, and BESS disconnection.

It is possible to observe how the BESSs are charged at almost its rating current in the LAB and power in the VRFB, followed by a resting period when BESSs are disconnected. Such operative action allows the limitation of the energy-charging costs in order to discharge this energy latter during the afternoon, improving the energy shifting process. Moreover, during the second valley period, between 13:48 pm and 18:24 pm, BESSs store a limited portion of energy to latter be discharge during the second peak-load between 18:24 pm, and 23:00 pm. Moreover, the maximum current ($I_{M(t)}$) and power ($P_{M(t)}$) per cell are adjusted at almost their rating values, suggesting that the solution is only based on the integer variables optimization, which could be a reasonable and simple operating policy results. However, the GA-GSA implementation proposed in this work extends the capabilities of GA-only method. Fig. 6 shows the voltage for both technologies, where it can be observed that the operating constraint (29) is successfully fulfilled since it is directly included on the simulation model.

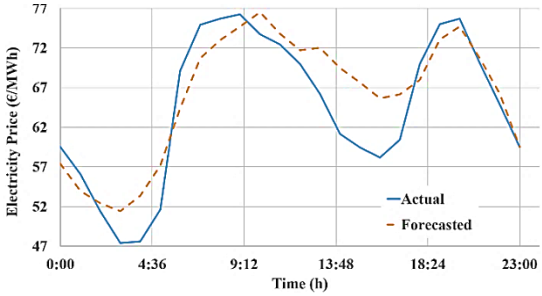

Figure 3. Actual and predicted electricity prices.

TABLE I. NET BENEFIT PER BESS TECHNOLOGY

	Predicted (€)	Actual (€)
BESS-LAB	-37.77	-38.10
BESS-VRFB	-17.41	-20.63

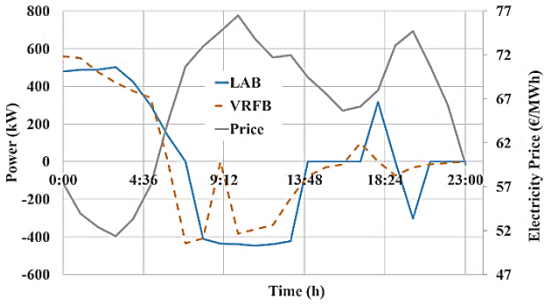

Figure 4. Charging and discharging power of BESS.

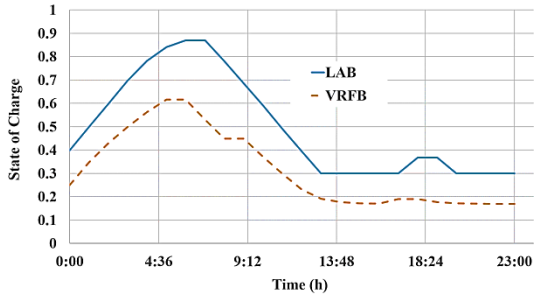

Figure 5. State of charge of BESS.

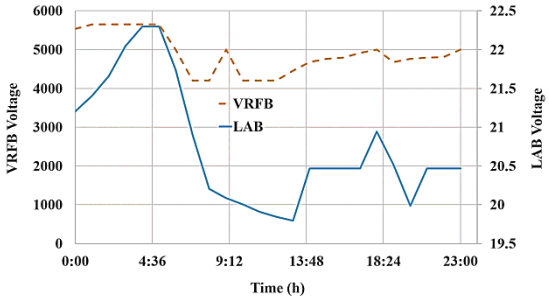

Figure 6. Voltage of BESS.

TABLE II. MAXIMUM CURRENT AND POWER BESS

Time (h)	$I_{M(t)}$ (A/cell) LAB		$P_{M(t)}$ (kW/cell) VRFB	
0:00	247.64	+1	3.38	+1
1:00	249.47	+1	4.92	+1
2:00	247.95	+1	3.65	+1
3:00	249.53	+1	4.90	+1
4:00	249.97	+1	4.93	+1
5:00	248.96	+1	4.64	+1
6:00	72.44	+1	0.00	0
7:00	0.00	0	4.72	–1
8:00	223.08	–1	4.90	–1
9:00	238.39	–1	0.00	0
10:00	240.56	–1	4.64	–1
11:00	246.21	–1	4.78	–1
12:00	242.71	–1	4.64	–1
13:00	249.56	–1	4.25	–1
14:00	245.48	–1	4.12	–1
15:00	0.00	0	4.99	–1
16:00	0.00	0	4.63	–1
17:00	0.00	0	0.54	+1
18:00	167.32	+1	0.00	0
19:00	0.00	0	4.93	–1
20:00	218.36	–1	4.88	–1
21:00	0.00	0	4.89	–1
22:00	238.05	–1	4.90	–1
23:00	245.54	–1	4.97	–1

VI. Conclusion

This work has introduced a methodological enhancement of an available technique for the management of BESS operating in real-time electricity markets based on GA, considering two technologies, LAB and VRFB, respectively, in order to consider the specific nonlinear features of each technology, whose have a considerable impact on the way how BESS and the grid interchange the power. The proposed model only optimizes the charging, discharging, and battery disconnection by means of integer variables, while the charging and discharging current and power remains constant at their maximum rates by means of the incorporation of GSA model. According to the results obtained from the case study, where the maximum current and power were suggested to be adjusted at their maximum rating values, the optimization analysis only considering the integer variables of the problem based on GA, which could offer a reasonable operating strategy. However, the GA-GSA combination proposed in this work offers a complete framework for the assessment of BESS-management with complex simulation models. If BESS acting as part of a virtual power plant participating electricity market, the forecasting of locational marginal price [20, 21], renewable power such as wind & solar [22-24] and aggregators [25-27] need to be considered during the joint dispatch scheduling so as to achieve optimal financial benefits.

VII. Acknowledgment

João P. S. Catalão acknowledges the support by FEDER funds through COMPETE 2020 and by Portuguese funds through FCT, under POCI-01-0145-FEDER-029803 (02/SAICT/2017). Gerardo J. Osório acknowledges the support by UIDB/00151/2020 research unit (C-MAST) funded by FCT.

References

[1] R. H. Byrne, T. A. Nguyen, D. A. Copp, B. R. Chalamala, I. Gyuk, "Energy management and optimization methods for grid energy storage systems," *IEEE Access*, vol. 6, pp. 13231-13260, Mar. 2018.

[2] T. Dragičević, H. Pandžić, D. Škrlec, I. Kuzle, J. M. Guerrero, D. S. Kirschen, "Capacity optimization of renewable energy sources and battery storage in an autonomous telecommunication facility," *IEEE Trans. Sustain. Energy*, vol. 5, pp. 1367-1378, Oct. 2014.

[3] S. A. Abdelrazek, S. Kamalasadan, "Integrated PV capacity firming and energy time shift battery energy storage management using energy-oriented optimization," *IEEE Trans. Ind. Appl.*, vol. 52, pp. 2607-2617, May/June 2016.

[4] P. B. L. Neto, O. R. Saavedra, L. A. d. S. Ribeiro, "A dual-battery storage bank configuration for isolated microgrids based on renewable sources," *IEEE Trans. Sustain. Energy*, vol. 9, pp. 1618-1626, Oct. 2018.

[5] Y. Jiang, L. Kang, Y. Liu, "A unified model to optimize configuration of battery energy storage systems with multiple types of batteries," *Energy*, vol. 176, pp. 552-560, June 2019.

[6] Q. Sun, D. Xing, H. Alafnan, X. Pei, M. Zhang, W. Yuan, "Design and test of a new two-stage control scheme for SMES-battery hybrid energy storage systems for microgrid applications," *Appl. Energy*, vol. 253, Nov. 2019.

[7] Y. Liu, Z. Li, Z. Lin, K. Zhao, Y. Zhu. "Multi-objective optimization of energy management strategy on hybrid energy storage system based on Radau pseudospectral method," *IEEE Access*, vol. 7, pp. 112483-112493, Aug. 2019.

[8] T. A. Nguyen, D. Copp, R. H. Byrne, B. Chalamala, "Market evaluation of energy storage systems incorporating technology-specific nonlinear models," *IEEE Trans. Power Syst.*, vol. 34, pp. 3706-3715, Apr. 2019.

[9] F. Sorourifar, V. M. Zavala, A. W. Dowling, "Integrated multiscale design, market participation, and replacement strategies for battery energy storage systems," *IEEE Trans. Sustain. Energy*, 2018, in press.

[10] A. Kumar, N. K. Meena, A. R. Singh, Y. Deng, X. He, R. C. Bansal, P. Kumar, "Strategic integration of battery energy storage systems with the provision of distributed ancillary services in active distribution systems," *Appl. Energy*, vol. 253, Nov. 2019.

[11] Y.-Y. Hong, M.-Y. Wu, "Markov model-based energy storage system planning in power systems," *IEEE Systems Journal*, 2019, in press.

[12] V.-H. Bui, A. Hussain, H.-M. Kim, "Double deep Q-learning-based distributed operation of battery energy storage system considering uncertainties," *IEEE Trans. on Smart Grid*, 2019, in press.

[13] J. M. Lujano-Rojas, R. Dufo-López, J. L. Bernal-Agustín, J. P. S. Catalão, "Optimizing daily operation of battery energy storage systems under real-time pricing schemes," *IEEE Trans. Smart Grid*, vol. 8, pp. 316-330, Jan. 2017.

[14] J. Schiffer, D. U. Sauer, H. Bindner, T. Cronin, P. Lundsager, R. Kaiser, "Model prediction for ranking lead-acid batteries according to expected lifetime in renewable energy systems and autonomous power-supply systems," *J. Power Sources*, vol. 168, pp. 66-78, May 2007.

[15] X. Qiu, T. A. Nguyen, J. D. Guggenberger, M. L. Crow, A. C. Elmore, "A field validated model of a vanadium redox flow battery for microgrids," *IEEE Trans. Smart Grid*, vol. 5, pp. 1592-1601, Jul. 2014.

[16] T. A. Nguyen, X. Qiu, J. D. Guggenberger II, M. L. Crow, A. C. Elmore, "Performance characterization for photovoltaic-vanadium redox battery microgrid systems," *IEEE Trans. Sustain. Energy*, vol. 5, pp. 1379-1388, Oct. 2014.

[17] T. A. Nguyen, M. L. Crow, A. C. Elmore, "Optimal sizing of a vanadium redox battery system for microgrid systems," *IEEE Trans. Sustain. Energy*, vol. 6, pp. 729-737, Jul. 2015.

[18] G. A. Rampinelli, A. Krenzinger, F. C. Romero, "Mathematical models for efficiency of inverters used in grid connected photovoltaic systems," *Renew. Sust. Energ. Rev.*, vol. 34, pp. 578-587, Jun. 2014.

[19] E. Rashedi, H. Hossein-pour, S. Saryazdi, "GSA: a gravitational search algorithm," *Inform. Sciences*, vol. 179, pp. 2232-2248, Jun. 2009.

[20] M. Liu, F.L. Quilumba, and W. Lee, "Dispatch Scheduling for a Wind Farm With Hybrid Energy Storage Based on Wind and LMP Forecasting," *IEEE Trans. Ind. Appl.*, vol. 51, no. 3, pp. 1970-1977, May-Jun. 2015.

[21] Z. Ding, W. Lee, and J. Wang, "Stochastic Resource Planning Strategy to Improve the Efficiency of Microgrid Operation," *IEEE Trans. Ind. Appl.*, vol. 51, no. 3, pp. 1978-1986, May-Jun. 2015.

[22] Y. Wu, P. Sun, T. Wu, J. Hong, and M.Y. Hassan, "Probabilistic Wind-Power Forecasting Using Weather Ensemble Models," *IEEE Trans. Ind. Appl.*, vol. 54, no. 6, pp. 5609-5620, Nov.-Dec. 2018.

[23] J. Ma, M. Yang, X. Han, and Z. Li, "Ultra-Short-Term Wind Generation Forecast Based on Multivariate Empirical Dynamic Modeling," *IEEE Trans. Ind. Appl.*, vol. 54, no. 2, pp. 1029-1038, Mar.-Apr. 2018.

[24] F. Wang, Z. Xuan, Z. Zhen, Y. Li, K. Li, L. Zhao, M. Shafie-khah, and J. P.S. Catalão, "A minutely solar irradiance forecasting method based on real-time sky image-irradiance mapping model," *Energy Convers. Manag.* vol. 220, Art. no. 113075, Sep. 2020.

[25] F. Wang, B. Xiang, K. Li, X. Ge, H. Lu, J. Lai, and P. Dehghanian, "Smart households' aggregated capacity forecasting for load aggregators under incentive-based demand response programs," *IEEE Trans. Ind. Appl.*, vol. 56, no. 2, pp. 1086-1097, Mar.-Apr. 2020.

[26] K. Li, F. Wang, Z. Mi, M. Fotuhi-Firuzabad, N. Dui, and T. Wang, "Capacity and output power estimation approach of individual behind-the-meter distributed photovoltaic system for demand response baseline estimation," *Appl. Energy*, vol. 253, Art. no. 113595, Nov. 2019.

[27] X. Lu, K. Li, H. Xu, F. Wang, Z. Zhou, and Y. Zhang, "Fundamentals and business model for resource aggregator of demand response in electricity markets," *Energy*, vol. 204, Art. no. 117885, May 2020.